Biosynthesis of Tropolones in *Streptomyces* spp.: Interweaving Biosynthesis and Degradation of Phenylacetic Acid and Hydroxylations on the Tropone Ring

Xuefei Chen,[a] Min Xu,[a] Jin Lü,[a] Jianguo Xu,[a] Yemin Wang,[a] Shuangjun Lin,[a] Zixin Deng,[a] Meifeng Tao[a]

[a] ▢ K L ▢ ▢ ▢ ▢ ▢ , J ▢ ▢ ▢ ▢ ▢ ▢ L ▢ ▢ ▢ ▢ ▢ D ▢ ▢ , ▢ ▢ ▢ ▢ ▢ L▢ ▢ ▢ ▢ B▢ ▢ ▢ , ▢ ▢ ▢▢▢ ▢ ▢ ▢, ▢ ▢ ▢ ▢ ▢ ▢ ▢ C ▢

Tropolonoids are important natural products that contain a unique seven-membered aromatic tropolone core and exhibit remarkable biological activities. 3,7-Dihydroxytropolone (DHT) isolated from *Streptomyces* species is a multiply hydroxylated tropolone exhibiting antimicrobial, anticancer, and antiviral activities. In this study, we determined the DHT biosynthetic pathway by heterologous expression, gene deletion, and biotransformation. Nine *trl* genes and some of the aerobic phenylacetic acid degradation pathway genes (*paa*) located outside the *trl* biosynthetic gene cluster are required for the heterologous production of DHT. The *trlA* gene encodes a single-domain protein homologous to the C-terminal enoyl coenzyme A (enoyl-CoA) hydratase domain of PaaZ. TrlA truncates the phenylacetic acid catabolic pathway and redirects it toward the formation of heptacyclic intermediates. TrlB is a 3-deoxy-D-arabino-heptulosonic acid-7-phosphate (DAHP) synthase homolog. TrlH is an unusual bifunctional protein bearing an N-terminal prephenate dehydratase domain and a C-terminal chorismate mutase domain. TrlB and TrlH enhanced *de novo* biosynthesis of phenylpyruvate, thereby providing abundant precursor for the prolific production of DHT in *Streptomyces* spp. Six seven-membered carbocyclic compounds were identified from the *trlC*, *trlD*, *trlE*, and *trlF* deletion mutants. Four of these chemicals, including 1,4,6-cycloheptatriene-1-carboxylic acid, tropone, tropolone, and 7-hydroxytropolone, were verified as key biosynthetic intermediates. TrlF is required for the conversion of 1,4,6-cycloheptatriene-1-carboxylic acid into tropone. The monooxygenases TrlE and TrlCD catalyze the regioselective hydroxylations of tropone to produce DHT. This study reveals a natural association of anabolism of chorismate and phenylpyruvate, catabolism of phenylacetic acid, and biosynthesis of tropolones in *Streptomyces* spp.

Tropolonoids are promising drug lead compounds because of the versatile bioactivities attributed to their highly oxidized seven-membered aromatic ring scaffolds. Our present study provides clear insight into the biosynthesis of 3,7-dihydroxytropolone (DHT) through the identification of key genes responsible for the formation and modification of the seven-membered aromatic core. We also reveal the intrinsic mechanism of elevated production of DHT and related tropolonoids in *Streptomyces* spp. The study on DHT biosynthesis in *Streptomyces* exhibits a good example of antibiotic production in which both anabolic and catabolic pathways of primary metabolism are interwoven into the biosynthesis of secondary metabolites. Furthermore, our study sets the stage for metabolic engineering of the biosynthetic pathway for natural tropolonoid products and provides alternative synthetic biology tools for engineering novel tropolonoids.

KEYWORDS *Streptomyces*, antibiotic, biosynthetic gene cluster, chorismate, natural products, phenylacetic acid, tropolone

he tropolonoid family of natural products, isolated from plants, fungi, and bacteria, is characterized by the presence of a cyclohepta-2,4,6-trienone moiety, a rare seven-membered nonbenzenoid aromatic ring named tropone (1). Hydroxylated tropones (i.e., tropolones) are known for their diverse bioactivities. Colchicine, β-thujaplicin (hinokitiol), stipitatic acid, and tropolone itself are the earliest reported representatives and were discovered from *Colchicum* species, *Thuja plicata* (*Chamaecyparis taiwanensis*), *Talaromyces stipitatus*, and *Penicillium aurantiobegii* ATCC 31099, respectively (1). Even very simple monocyclic tropolones exhibit broad bioactivities. For example, as the simplest tropolone, tropolone itself is used as an iron transporter in serum-free medium for animal cell culturing (3), while it was discovered as a virulent factor of the plant pathogen *Burkholderia plantarii*, causing rice seedling blight (4). The α-hydroxyl group is necessary for the ion-chelating and biological activities of tropolone. 3,7-Dihydroxytropolone (compound 1 [see Fig. 1A]), isolated from *Streptomyces* sp. *flavus*, is a multiply hydroxylated tropolone exhibiting strong antimicrobial, antitumor, and antiviral activities (5). The contiguous array of at least three oxygen atoms (ketone/hydroxyl) and the seven-membered aromatic ring are both essential for the broad bioactivities of compound 1 (6, 7). Interest in the potential bioactivities and unusual structure of compound 1 has generated a number of chemical synthesis studies focused on the derivatization of tropolone, as well as studies supporting tropolone as a very promising therapeutic drug lead (2, 8–10).

Previous biosynthetic studies of tropolonoids have revealed diverse routes for the formation of the tropone ring, all involving a key ring expansion step from a benzenoid framework (11). In *Talaromyces stipitatus*, stipitatic acid is produced through a nonreducing polyketide synthase (NR-PKS) pathway. The tropolone core of stipitatic acid is generated via a pinacol-type rearrangement catalyzed by a nonheme Fe(II)-dependent dioxygenase, TropC (12). In prokaryotes, two pathways have been proposed for the biosynthesis of tropolonoids. A type II polyketide assembly line followed by predicted complex oxidative rearrangements is responsible for the biosynthesis of rubrolones in *Streptomyces* spp. (13). *Escherichia coli* is not known to produce tropolonoid, but it has an unorthodox aerobic phenylacetic acid (PAA) catabolic pathway that degrades PAA via a ring epoxide-oxepin rearrangement followed by PaaZ-catalyzed hydrolytic ring cleavage and oxidation. *In vivo* data suggested that when the oxidation function of PaaZ was deficient, the aerobic PAA catabolic pathway was truncated and branched to the production of 2-hydroxycyclohepta-1,4,6-triene-1-formyl-CoA, which is proposed as a long-sought seven-membered carbocyclic intermediate for the biosynthesis of bacterial tropolonoids (14, 15). This aerobic PAA degradation pathway is widespread in bacteria (15) and was recently found to be required for the biosynthesis of tropodithietic acid (TDA) and roseobacticide in *Phaeobacter inhibens* (16, 17).

Streptomyces species are the producers of many important secondary metabolites. Besides the polyketide-derived multicyclic tropolonoids, such as rubrolones, some *Streptomyces* strains produce small tropolonoids, such as compound 1 (5). During our ongoing antibiotic-screening program, we discovered that two *Streptomyces* strains, *Streptomyces cyaneofuscatus* Soc7 and *Streptomyces luteogriseus* Slg41, produced compound 1 at very high titers compared to those reported in the literature. In this work, we sought to study the biosynthesis of compound 1 to reveal the formation of the tropone core, the multiple hydroxylations on the seven-membered aromatic ring, and the mechanism of the high yield of compound 1.

Streptomyces *.* *S. cyaneofuscatus* Soc7 and *S. luteogriseus* Slg41 produced 3,7-dihydroxytropolone (compound 1) (Fig. 1A) at high titers (380 and 230 mg/liter, respectively), which were >10,000-fold higher than the titer reported for *S. flavus* No. K611-97, the species from which compound 1 was first identified (5). The identity of compound 1 was confirmed by nuclear magnetic resonance (NMR), high-resolution mass spectrometry (HRMS), and X-ray crystallography (Fig. 1B). To isolate the
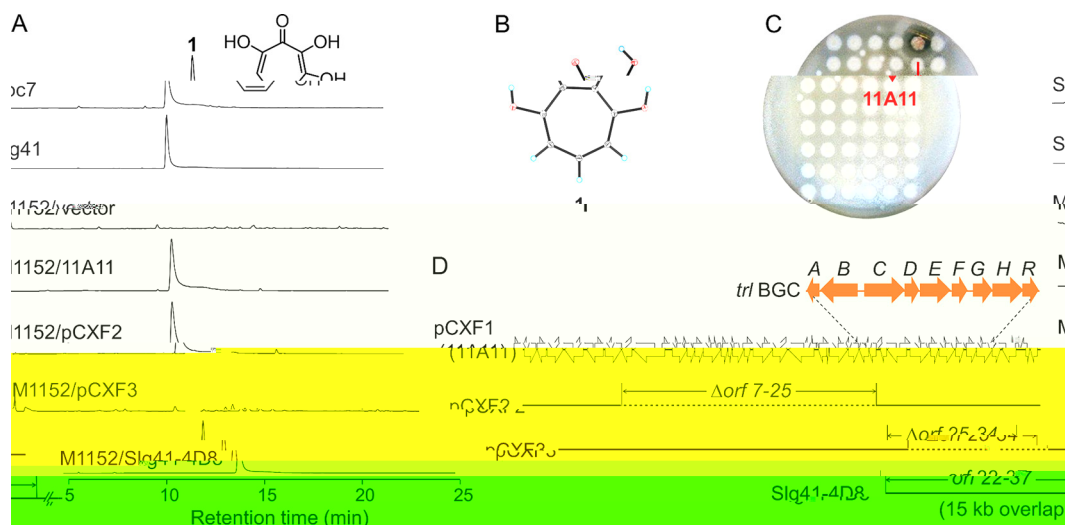
Identification of 3,7-dihydroxytropolone (compound 1) and its biosynthetic gene cluster. (A) HPLC analysis of the production of compound 1 in two natural *Streptomyces* strains, *S. cattleya* Soc7 and *S. luteireticuli* Slg41, and in heterologous expression strains. The structure of compound 1 is shown at the upper right. M1152, *S. coelicolor* M1152; vector, pJTU2554. Compound 1 was eluted at 14 min in the HPLC, as shown. HPLC was monitored at 254 nm. (B) X-ray crystal structure of compound 1. (C) Cloning of the BGC of compound 1 using the bioactivity-guided library expression and analysis (LEXAS) approach. Cosmid clone 11A11 was identified by its ability to inhibit the growth of *B. subtilis*. (D) DNA inserts of the cosmids and derivatives carrying chromosomal regions surrounding the *trl* BGC. Wide arrows represent open reading frames; solid lines, DNA inserts; dotted lines, deleted regions. Only part of the Slg41-4D8 insert is shown.

biosynthetic gene cluster (BGC) for compound 1, we used a recently established high-throughput library expression and bioactivity-guided screening approach, LEXAS (18). LEXAS screening of the genomic library of *S. cattleya* Soc7 yielded a positive cosmid clone, 11A11, whose exconjugant on the fermentation agar petri dish produced a clear zone of *Bacillus subtilis* growth inhibition (Fig. 1C). To confirm the screening result, cosmid DNA of 11A11 was introduced into *Streptomyces coelicolor* M1152 and *S. coelicolor* M1154 for heterologous expression. The production of compound 1 was detected in the resulting exconjugants by high-performance liquid chromatography (HPLC) analysis; *S. coelicolor* M1152/11A11 is shown as an example in Fig. 1A. Heterologous production of compound 1 reached high titers of 606 and 498 mg/liter in *S. coelicolor* M1152/11A11 and M1154/11A11, respectively. These results indicated that 11A11 contained the complete BGC for the heterologous biosynthesis of compound 1. For consistency with its subsequently derived constructs, cosmid 11A11 was named pCXF1. In subsequent genetic studies, *S. coelicolor* M1152/pCXF1 was used as the wild type and the parent strain for the construction of large-fragment deletion and in-frame deletion mutants.

Cosmid pCXF1 was sequenced, and bioinformatics analysis of the 39-kb insert revealed 37 open reading frames (ORFs) (Fig. 1D), including two clusters of genes related to riboflavin biosynthesis (*orf8* to *orf18*) and aromatic metabolism (*orf26* to *orf34*), respectively. To identify genes responsible for the biosynthesis of compound 1, two regions were deleted from pCXF1: one deletion, spanning *orf7* to *orf25*, removed the riboflavin biosynthesis region and resulted in pCXF2, and the other deletion, spanning *orf25* to *orf34*, removed the aromatic metabolism region and resulted in pCXF3 (Fig. 1D). HPLC analysis indicated that the production of compound 1 was maintained in *S. coelicolor* M1152/pCXF2 but not in *S. coelicolor* M1152/pCXF3 (Fig. 1A), suggesting that the genes missing from pCXF3 were required for heterologous production of compound 1. In addition, another compound 1-producing clone, Slg41-4D8, was obtained from the LEXAS screening of the *S. luteireticuli* Slg41 genomic library. Sequencing revealed that Slg41-4D8 had a 15-kb DNA overlapping and identical with the *orf22*-to-*orf37* region of pCXF1 (Fig. 1D). These results indicated that *orf1* to *orf25* were not required, and that *orf26* to *orf34* were required, for the production of compound 1. Three other genes at the
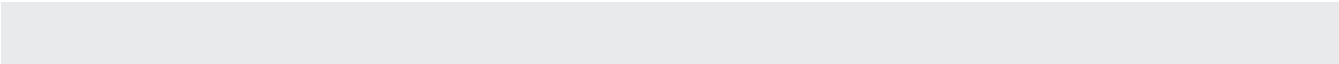
right boundary of pCXF1, *f35* to *f37*, encode transcriptional regulators and thus are not directly involved in the biosynthesis of compound 1.

trl. The nine genes required for the biosynthesis of compound 1 were renamed *trlABCDEFGHR*. These *trl* genes are organized into three putative operons: *trlAB*, *trlCDEF*, and *trlGHR* (Fig. 1D). TrlA contains a MaoC dehydratase domain and is similar to the enoyl coenzyme A (enoyl-CoA) hydratase domain of *E. coli* bifunctional protein PaaZ (similarity, 47%; identity, 31%). *E. coli* PaaZ is a key catabolic enzyme involved in the aerobic degradation of PAA. PaaZ contains an N-terminal aldehyde dehydrogenase (ALDH) domain and a C-terminal (*R*)-specific enoyl-CoA hydratase domain (ECH). PaaZ ECH is responsible for the hydrolytic ring cleavage of oxepin-CoA to generate a highly reactive 3-oxo-5,6-dehydrosuberyl-CoA semialdehyde in *E. coli* (14). The ALDH domain is responsible for further oxidation of that semialdehyde into 3-oxo-5,6-dehydrosuberyl-CoA. With the help of other catabolic enzymes, 3-oxo-5,6-dehydrosuberyl-CoA is broken down into two acetyl-CoA molecules and one succinyl-CoA molecule (15). In the absence of a functional ALDH domain, the aerobic PAA degradation pathway is blocked at the semialdehyde (14). In this case, the semialdehyde undergoes spontaneous intramolecular Knoevenagel condensation and dehydration to yield 2-hydroxycyclohepta-1,4,6-triene-1-formyl-CoA (14), which is proposed to be the long-sought intermediate for the production of seven-membered carbocyclic antibiotics, such as TDA and roseobacticide in *P. inhibe* (14, 16, 17). Interestingly, there is no ALDH domain in TrlA, implying a truncated PAA catabolic pathway.

TrlB is homologous to 3-deoxy-D-arabino-heptulosonic acid-7-phosphate (DAHP) synthase, catalyzing the condensation of phosphoenolpyruvate and D-erythrose-4-phosphate to generate DAHP, which is the first committed step of the shikimate biosynthetic pathway. TrlH is a bifunctional protein bearing an N-terminal prephenate dehydratase (PDT) domain and a C-terminal chorismate mutase (CM) domain, which exhibits an unusual domain arrangement, opposite that of the bifunctional P-protein in Gram-negative bacteria (19). P-protein bears an N-terminal CM domain and a C-terminal PDT domain that convert chorismate into prephenate and phenylpyruvate sequentially. The *trlG* and *trlR* genes form one operon with *trlH*. TrlG is an unknown protein bearing an AfsA-like hotdog-fold protein domain, while TrlR is a TetR family transcriptional regulator.

TrlC and TrlD are homologous to the HpaB superfamily oxidase component and the HpaC superfamily flavin reductase component of 4-hydroxyphenylacetate 3-monooxygenase, respectively. HpaB and HpaC in *E. coli* make up a two-component monooxygenase with aromatic hydroxylase activity (20). Therefore, TrlC and TrlD were proposed to function as a two-component monooxygenase named TrlCD. TrlE is a monooxygenase homolog of flavin adenine dinucleotide (FAD)-dependent 6-hydroxynicotinate 3-monooxygenase (similarity, 46%; identity, 33%) (21). The *trlF* gene product is an unknown protein similar to the carnitine operon protein CaiE of *Salmonella enterica* (similarity, 74%; identity, 58%) and *E. coli* K-12 (similarity, 75%; identity, 55%) (22) and less similar to the unknown protein PaaY of the PAA degradation gene cluster in *E. coli* (similarity, 65%; identity, 50%) (23). Information about the Trl proteins encoded by the *trl* BGC, including their deduced functions, is summarized in Table 1.

. To determine whether the *paaZ* ECH-homologous gene *trlA* is involved in the biosynthesis of compound 1, *trlA* was deleted from pCXF1 to produce pCXF4, which was introduced into *S. coelicolor* M1152 to yield the in-frame deletion mutant *S. coelicolor* M1152/pCXF4 (i.e., the Δ*trlA* mutant) (see Fig. S1 in the supplemental material). HPLC-mass spectrometry (MS) analysis of the Δ*trlA* ferment revealed that compound 1 production was abolished and that PAA (compound 2) accumulated (Fig. 2A), indicating that *trlA* is required for compound 1 production and implying that compound 1 originates from compound 2. This result also implied that TrlA directs the cellular PAA catabolic pathway toward the biosynthesis of compound 1, as proposed for other tropolonoids (14). However, there is no other gene in the *trl*

BGC that shares similarity with the early bacterial aerobic PAA catabolic genes. We therefore speculated that the endogenous *paa* genes from the *S. coelicolor* surrogate host participated in the biosynthesis of compound 1—for example, *SCO7471* to *SCO7475*, which form an operon orthologous to the *E. coli paaABCDE* operon encoding subunits of the monooxygenase (epoxidase) complex responsible for the oxidation of PAA-CoA to epoxy-ring-1,2-phenylacetyl-CoA. To test this hypothesis, *SCO7471* to *SCO7475* were deleted from the *S. coelicolor*

biosynthesis of compound 1. Other *aa*-homologous genes in the *S. c elic l* genome, including those encoding the PAA-CoA ligase PaaK (*SCO7469*) and enoyl-CoA isomerase PaaG (*SCO5144*), which catalyze early steps of the aerobic PAA catabolic pathway (15), should also be involved in the biosynthesis of compound 1.

, , , de novo

Streptomyces. The sequences of TrlB and TrlH suggested their key roles in the supply of PAA precursor for the biosynthesis of compound 1. To investigate their roles in compound 1 biosynthesis, *trlB* and *trlH* were deleted from pCXF1, and the resulting plasmids were introduced into *S. c elic l* M1152 to yield two in-frame deletion mutant strains, the Δ*trlB* and Δ*trlH* strains, respectively. HPLC analysis revealed a deficiency in compound 1 production in the two mutants (Fig. 3). In addition, the Δ*trlH* mutant accumulated a large amount of 3-[(1-carboxyethenyl)oxy]benzoic acid (compound 3) and smaller amounts of other chorismate-derived metabolites, such as anthranilic acid (compound 4), 4-hydroxyphenylacetic acid (compound 5), 2-acetamido-5-hydrobenzoic acid (compound 6), and phenylpyruvic acid (compound 7) (Fig. 3). The chemical identities of compounds 3 to 7 were determined by HRMS and/or NMR analyses (see Table S1 in the supplemental material). These aromatic compounds could be derived from the common precursor chorismate, through different pathways (19, 24–26). These findings supported the notion that TrlB and TrlH contributed to the biosynthesis of compound 1 by providing a rich source of precursor through boosting the shikimate pathway (by TrlB) and converting chorismate to compound 7 (by TrlH).

To further confirm the contribution of TrlB and TrlH to the production of compound 7, *trlB* and *trlH* were expressed in *E. c li* BL21(DE3). Isopropyl β-D-1-thiogalactopyranoside (IPTG)-induced *E. c li* cultures were extracted and were analyzed by HPLC. Massive accumulation of compound 7 was observed in the extract of *E. c li* expressing TrlB alone (4.02 mg/liter) or TrlB and TrlH together (6.72 mg/liter), in contrast to accumulation in the vector control strains (0.046 mg/liter and 0.042 mg/liter) (see Fig. S2 in the supplemental material). These data supported the notion that TrlB and TrlH enhanced the biosynthesis of compound 7 and thereby contributed to the high yield of compound 1 in the heterologous hosts and in the natural strains *S. c a e f cq* Soc7 and *S. l egie* Slg41. These two natural strains produced compound 1 at a >10,000-fold-higher yield than that of
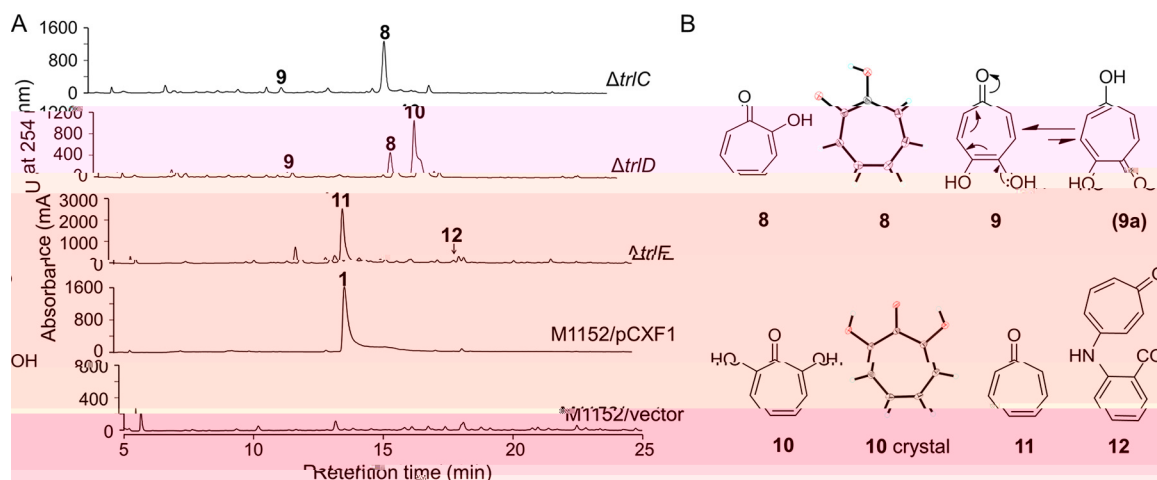
FIG 4 Metabolic analysis of the ΔtrlC, ΔtrlD, and ΔtrlE mutants and chemical structures of the accumulated compounds. (A) HPLC analysis of *S. coelicolor* M1152/pCXF1 and trl gene deletion mutants. Vector, pJTU2554. (B) Structures of the accumulated compounds. The X-ray crystal structures of compounds 8 and 10 are also shown. The products identified were as follows: tropolone (compound 8), 4,5-dihydroxytropone (compound 9), 7-hydroxytropolone (compound 10), tropone (compound 11), and 2-(1,3,6-cycloheptatriene-5-oxo)-aminobenzoic acid (compound 12). Compounds 9 and 12 are discovered here as natural products.

the producer originally isolated, *S. tropica* No. K611-97, from which 4 mg of the compound was purified from 208 liters of liquid culture (5). To determine whether compound 7 is the on-pathway intermediate to compound 1, a biotransformation experiment was performed by feeding compound 7 to the ΔtrlB mutant. As expected, the production of compound 1 was clearly observed in the HPLC (see Fig. S3 in the supplemental material).

In-frame deletion mutants *S. coelicolor* M1152/pCXF10 (i.e., the ΔtrlG mutant) and *S. coelicolor* M1152/pCXF12 (i.e., the ΔtrlR mutant) were constructed, and HPLC analysis indicated that these mutants also lacked compound 1 production and accumulated compounds 3 to 7. Both the ΔtrlG mutant and the ΔtrlR mutant showed HPLC profiles similar to that of the ΔtrlH mutant, except that the absorbance peaks in the ΔtrlG and ΔtrlR mutants were much lower than their counterparts in the ΔtrlH mutant (Fig. 3A). These results suggested that TrlR regulated the expression of TrlG and TrlH and that TrlG played a pivotal role in precursor supply for the biosynthesis of compound 1.

Characterization of the trlC-to-trlE gene products. To investigate the hydroxylation modifications on the tropone ring that lead to the multiply hydroxylated product compound 1, the two-component monooxygenase genes trlC and trlD and the other monooxygenase gene, trlE, were deleted in pCXF1 and were introduced into *S. coelicolor* M1152 to yield three in-frame deletion mutants: *S. coelicolor* M1152/pCXF6 (ΔtrlC), *S. coelicolor* M1152/pCXF7 (ΔtrlD), and *S. coelicolor* M1152/pCXF8 (ΔtrlE). The ΔtrlC mutant lost the production of compound 1 and accumulated two compounds that were identified as tropolone (compound 8) and 4,5-dihydroxytropone (compound 9) through X-ray crystallography, HRMS, and NMR analyses (Fig. 4; see also Table S2 in the supplemental material). Compound 9 may be regarded as a tautomer of 2,5-dihydroxycyclohepta-2,4,6-trienone (compound 9a), which is a synthesized chemical (27). The ΔtrlD mutant also lost the production of compound 1 and accumulated compounds 8 and 9. In addition, this mutant accumulated another major component, which was characterized as 7-hydroxytropolone (compound 10) through HRMS, X-ray crystallography, and NMR analyses (Fig. 4; also Table S2). Mutation of trlE abolished the production of compound 1, and the ΔtrlE mutant accumulated two different compounds, identified as tropone (compound 11) and 2-(1,3,6-cycloheptatriene-5-oxo)-aminobenzoic acid (compound 12) (Fig. 4; also Table S2). Compound 12 is a novel tropone natural product. The production of compound 9 in both the ΔtrlC and ΔtrlD mutants implied the presence of an unknown hydroxylation enzyme. The production of compound 12 in the ΔtrlE
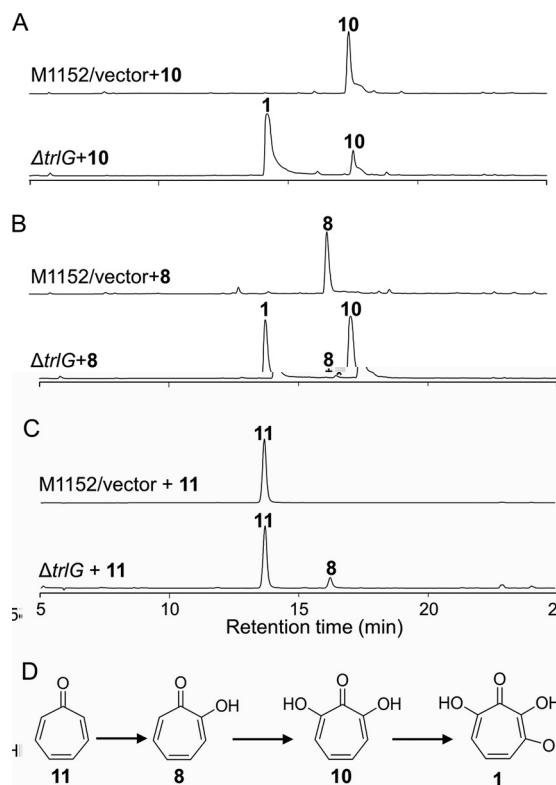
FIG 5 Transformation of tropone or tropolones by feeding to *Streptomyces* cultures or by incubation with *Streptomyces* cell extracts. (A) HPLC detection of the biotransformation of compound 10 after feeding to a culture of the Δ*trlG* mutant (*S. coelicolor* M1152/pCXF10) or the vector control. HPLC was monitored at 254 nm. (B) HPLC detection of the biotransformation of compound 8 after feeding to a culture of the Δ*trlG* mutant or the vector control. HPLC was monitored at 254 nm. (C) HPLC detection of the biotransformation of compound 11 after incubation with a cell extract of the Δ*trlG* mutant or the vector control. HPLC was monitored at 300 nm. (D) Schematic representation of biotransformations of compound 11 through compounds 8 and 10 to compound 1.

mutant is also a mystery, although a substitution by anthranilic acid at C-4 or C-5 is possible, owing to the cycloheptatrienylium ion nature of tropone (28). Nevertheless, compounds 9 and 12 are minor components and are probably shunt products.

To determine whether compounds 11, 8, and 10 are real biosynthetic intermediates, biotransformation experiments were performed by feeding these compounds to the Δ*trlG* mutant and/or incubating them with cell extracts of the Δ*trlG* mutant. The Δ*trlG* mutant carries functional genes for the production of TrlC, TrlD, and TrlE. Feeding compound 10 to the Δ*trlG* mutant resulted in the production of compound 1, suggesting that compound 1 is synthesized from the hydroxylation of C-3 on compound 10 (Fig. 5A). Feeding compound 8 to the Δ*trlG* mutant resulted in the production of compound 10, and prolonged incubation resulted in the production of compound 1 (Fig. 5B), suggesting that compound 10 is synthesized from the hydroxylation at C-7 of compound 8. However, no biotransformation was observed for compound 11 in the feeding experiment, which could be explained by the poor uptake of compound 11 by bacterial cells. To overcome the potential uptake problem with compound 11, a cell extract of the Δ*trlG* mutant was incubated with compound 11. As expected, conversion of compound 11 to compound 8 was clearly observed in the HPLC (Fig. 5C). These results indicated that compound 1 is produced from compound 11 via successive hydroxylations, first at its C-2 site to yield compound 8, in a reaction catalyzed by TrlE, and then at its C-7 and C-3 sites to yield compounds 10 and 1, in reactions catalyzed by the two-component monooxygenase TrlCD (Fig. 5D).

To confirm that TrlE catalyzes the conversion of compound 11 to compound 8, a biotransformation experiment was conducted with cell extracts of an *E. coli* strain
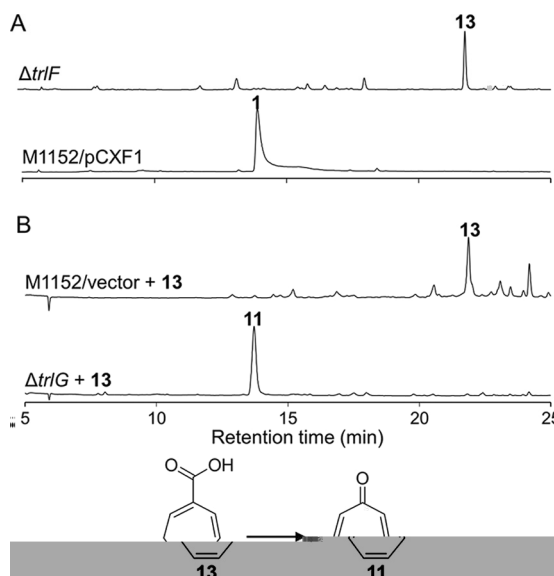
HPLC analysis of the Δ*trlF* mutant and biotransformation of the accumulated compound 13. (A) HPLC analysis of *S. c elic l* M1152/pCXF1 and the *trlF* gene deletion mutant (*S. c elic l* M1152/pCXF9). HPLC was monitored at 254 nm. (B) HPLC detection of the biotransformation of compound 13 (cyclohepta-1,4,6-triene-1-carboxylic acid) after incubation with a cell extract of the Δ*trlG* mutant (*S. c elic l* M1152/pCXF10) or the vector control. HPLC was monitored at 300 nm.

expressing TrlE. The *E. c li* cell extract was incubated with compound 11 at 30°C for 2 h. Conversion of compound 11 to compound 8 was clearly observed from the HPLC (see Fig. S4 in the supplemental material), confirming that the monooxygenase TrlE was responsible for C-2 hydroxylation on compound 11 to generate compound 8. To confirm that TrlCD catalyze the conversions of compound 8 to compound 10 and of compound 10 to compound 1, TrlC and TrlD were expressed in *E. c li* BL21(DE3). The cell extracts were incubated with compound 8 or compound 10 at 30°C for 2 h. A stepwise conversion of compound 8 to compound 10 and compound 1 was clearly observed from the HPLCs (see Fig. S5 in the supplemental material), confirming that the two-component monooxygenase TrlCD was responsible for the C-7 and C-3 hydroxylations on compound 8 to give the final product, compound 1.

1,4,6-cyclohept triene-1-c rboxylic cid is bios nthetic intermedi te for compound 1. The *trlF* deletion also resulted in the abolishment of compound 1. To our surprise, the Δ*trlF* mutant (*S. c elic l* M1152/pCXF9) accumulated a novel compound (Fig. 6A), which was elucidated as 1,4,6-cycloheptatriene-1-carboxylic acid (compound 13) using HRMS and NMR analyses (Table S2 in the supplemental material). To determine whether compound 13 is a biosynthetic intermediate for compound 1, a cell extract of the Δ*trlG* mutant was mixed with compound 13 as a substrate and was incubated at 30°C for 2 h. HPLC analysis of the cell-free reaction mixture indicated that compound 13 was completely converted to compound 11 (Fig. 6B), suggesting that compound 13 is a bona fide biosynthetic intermediate of compound 1.

P A ori in of tropolone r n bios nthesis in *Strept m ces* spp. The involvement of the PaaZ ECH and PaaABCDE homologs in the biosynthesis of compound 1 clearly supports a PAA origin for compound 1 in *Strep tom ce* spp., a feature similar to that in *P. i hibe*, in which a specific didomain enzyme, PaaZ2, was found to be required for the production of TDA and roseobacticide (16, 17). PaaZ2 is a didomain protein homologous to *E. c li* PaaZ, but it carries C295R and E256C mutations in the active sites and therefore likely inactivates its ALDH function (16, 17). In *E. c li*, when the oxidization activity of the PaaZ ALDH domain was abolished, PAA degradation was blocked, and the truncated PAA catabolism produced 2-hydroxycyclohepta-

1,4,6-triene-1-formyl-CoA (14). This CoA thioester was proposed as a plausible biosynthetic intermediate for the production of TDA and other bacterial tropolonoids (14). Our genetic data suggested that a truncated PAA degradation pathway is required to construct the seven-membered carbocyclic scaffold of compound 1 in *Streptomyces* spp., where a single domain (ECH) protein, TrlA, plays a pivotal role in redirecting the degradation pathway.

The DAHP synthase gene homolog TrlB and the bifunctional protein TrlH (with prephenate dehydratase and chorismate mutase fused) are key enzymes of the chorismate and phenylpyruvate biosynthetic pathways. The involvement of TrlB and TrlH in the production of compound 1 also supported the notion that compound 1 is derived from compound 2, which is, however, supplied through anabolic reactions in this case, and indicated a strong connection between primary and secondary metabolism. Obviously, the *trlB* and *trlH* genes accounted for the high yield of compound 1 in *Streptomyces* spp. by supplying sufficient amounts of PAA precursor. The chromosomal genes of the heterologous expression host *S. coelicolor* also encode TrlB- and TrlH-like enzymes for the synthesis and utilization of chorismate, i.e., DAHP synthase (SCO2115), prephenate dehydratase (SCO3962), and chorismate mutase (SCO1762, SCO2019, and SCO4784), which are crucial for the normal growth of the strain. Interestingly, however, both the Δ*trlB* and the Δ*trlH* mutant lost production of compound 1, indicating that the genes mentioned above do not contribute significantly to the production of compound 1.

Notably, TrlH is a unique bifunctional PDT-CM protein in Gram-positive bacteria, and its domain organization contrasts with that of the bifunctional P-protein (CM-PDT) of Gram-negative bacteria (19). P-protein is a key regulation node for fine-tuning metabolic flow into the phenylalanine synthetic pathway in bacteria. P-protein is allosterically retroinhibited by L-Phe, and the two highly conserved motifs GAL/V and ERRP have been identified as essential for L-Phe binding to the regulatory domain (19). Interestingly, TrlH does not contain any conserved L-Phe binding motifs. However, several benzenoids found in the Δ*trlH* mutant, such as compounds 3 to 6, were also found to be accumulated in another mutant, the Δ*trlG* mutant, implying that TrlH may be subjected to feedback inhibition by a yet unknown metabolite. TrlG is an unknown protein required for precursor supply for the biosynthesis of compound 1. TrlG might

in *Alicyclobacillus acidiphilus* (31), and tropone (compound 11) has been reported from *Arachidnia* and marine bacteria of the *Roseobacter* clade as a natural product or shunt (16, 32, 33). Given the wide distribution of *vaa* genes and *tIF* homologs in bacteria, the distribution and diversity of tropone-derived metabolites may have been underestimated. Furthermore, the *tI* genes found in this study could be used to discover new tropolonoids, for example, via synthetic biology technologies.

. *E. coli* DH10B was used as a host for general DNA cloning, and *E. coli* XL1-Blue MR/pUZ8002 was used for construction of the cosmid genomic library (34). *E. coli* BW25113/pIJ790 was used for λ Red-mediated PCR targeting to construct gene disruption mutants (35, 36). *E. coli* BT340 (*E. coli* DH5α/pCP20) was used for the construction of in-frame deletion mutants using flippase recombination enzyme (FLP)-mediated site-specific recombination (36). *E. coli* ET12567/pUB307 was used as the helper strain to facilitate *E. coli–Streptomyces* intergenus triparental mating (37), and *E. coli* BL21(DE3) (Novagen) was used for protein expression. *S. scaefocqus* Soc7 and *S. lycegies* Slg41

plasmids (cosmids and related gene disruption mutants) can be mobilized into *Streptomyces* spp. and integrated site-specifically into the chromosome at the $\phi B_{\phi C31}$ attachment site. pJTU6722 (41) was used for amplifying the erythromycin resistance gene *ermB* flanked by the FLP recombination target (FRT) sequence in λ-Red-mediated PCR targeting. pET-28a (Novagen), pSUMO (42), and pSJ7 (43) were used for soluble protein expression. The oligonucleotides used in this study are listed in Table 2.

**. Luria-Bertani (LB) medium was used for *E. coli* growth. MS medium (44), containing, per liter, 20 g soybean flour, 20 g mannitol, and 20 g agar (pH 7.2 to 7.4) was used for *Streptomyces* growth, sporulation, and conjugation. R3 medium (45), containing, per liter, 10 g glucose, 5 g yeast extract, 0.1 g Casamino Acids, 3 g L-proline, 10 g MgCl$_2$·6H$_2$O, 4 g CaCl$_2$·2H$_2$O, 0.25 g K$_2$SO$_4$, 0.05 g KH$_2$PO$_4$, 5.6 g 2-[Tris(hydroxymethyl)-methylamino]-ethanesulfonic acid (TES), and 2 ml trace element solution (pH 7.2), was used for *Streptomyces* fermentation. The trace element solution was composed of ZnCl$_2$ (40 mg), FeCl$_3$·6H$_2$O (200 mg), CuCl$_2$·2H$_2$O (10 mg), MnCl$_2$·4H$_2$O (10 mg), Na$_2$B$_4$O$_7$·10H$_2$O (10 mg), and (NH$_4$)$_2$Mo$_7$O$_{24}$·4H$_2$O (10 mg) dissolved in 1 liter of double-distilled water (ddH$_2$O). TSBY medium (44), containing, per liter, 30 g tryptone soy broth (TSB; Oxoid), 103 g sucrose, and 5 g yeast extract, was used to inoculate *Streptomyces* mycelium for genomic DNA extraction and seeding.

**. β-Thujaplicin (hinokitiol) was purchased from Tokyo Chemical Industry (TCI). Antibiotics used in this study were purchased from Amresco; restriction enzymes were purchased from Fermentas (Thermo Fisher Scientific), and the cosmid library production kit was purchased from Epicentre (catalog no. CCFOS110). Oligonucleotides were synthesized, and DNA sequencing was performed, by Jie Li Biology Co. Ltd. *Taq* DNA polymerase and *Pfu* DNA polymerase were purchased from Vazyme Biotech and Yeasen Biotech, respectively. Gel extraction and plasmid isolation kits were purchased from Omega Bio-tek.

**. The cosmid library of *S. cattleya* Soc7 was constructed as described previously (34). High-molecular-weight genomic DNA (~200 kb) of *S. cattleya* Soc7 was partially digested with Sau3AI and was then recovered for ligation with HpaI- and BamHI-digested pJTU2554 (40). MaxPlax lambda packaging extracts were used to package the ligation mixture and to transfect *E. coli* XL1-Blue MR/pUZ8002 competent cells (34), resulting in a genomic library with approximately 2,000 clones that were stored in 20 96-well plates at −80°C. The identical procedure was used to construct the cosmid genomic library of *S. coelicolor* M145, using SuperCos 1 as the vector.

A bioactivity-guided high-throughput library expression approach was used to identify the biosynthetic gene cluster for compound 1 as described previously (18). The *S. cattleya* Soc7 cosmid genomic library was inoculated into 96-well plates (130 μl/well) at 37°C and 220 rpm for 4 to 6 h until growth reached an optical density at 600 nm (OD$_{600}$) of 0.4 to 0.6. The *E. coli* cultures were then transferred to SFM plates (44) (supplemented with 20 mM MgSO$_4$) precoated with heat-activated *S. lividans* SBT5 spores (a 48-pin replicator was used to transfer the cosmids into *S. lividans* SBT5). *S. lividans* SBT5/cosmid exconjugants were selected by flooding with apramycin (50 mg/liter) and trimethoprim (50 mg/liter), resulting in an expression library. The expression library was propagated in R3 medium at 28°C to 30°C for 4 to 6 days, followed by overlaying with *B. subtilis* and then culturing at 37°C for 16 to 24 h. Exconjugant 11A11, which showed antibacterial activity, was selected for further study.

-. The 11A11 cosmid (pCXF1) identified was transferred into *S. coelicolor* M1152 using *E. coli*-*Streptomyces* interspecies triparental mating, as described previously, for heterologous expression (44). *S. coelicolor* M1152/pCXF1 was selected and was then propagated in R3 medium for the production of compound 1. Meanwhile, pCXF1 was also isolated and sequenced at the China National Human Genome Centre at Shanghai, resulting in a 39-kb DNA sequence predicted to bear two clusters of genes responsible for riboflavin biosynthesis and shikimate metabolism, respectively.

λ-Red-mediated PCR targeting technology was used to construct Δ*orf7*-to-*orf25* (Δ*rib*) and Δ*orf25*-to-*orf34* (Δ*shi*) gene deletion mutants (36). PCR-targeting primers Δrib-F/Δrib-R (Δrib-F/R) and Δshi-F/R were used to amplify an erythromycin resistance gene cassette (*ermB*) from pJTU6722 (41) flanked by FLP recognition sites. The PCR products of the erythromycin resistance gene cassette were purified and were used to transform *E. coli* BW25113/pIJ790/pCXF1 competent cells by electroporation so as to replace *orf7* to *orf25* or *orf25* to *orf34* in pCXF1. The gene replacement constructs were then introduced into *E. coli* BT340, which was cultured at 42°C to remove the *ermB* cassette by FLP-mediated excision with an 81-bp scar remaining, resulting in constructs pCXF2 and pCXF3. The gene deletion constructs were confirmed by PCR analysis with primers ver-Δrib-F/R and ver-Δshi-F/R and by DNA sequencing. Finally, pCXF2 and pCXF3 were introduced into *S. coelicolor* M1152 individually by *E. coli*-*Streptomyces* triparental mating to integrate them into the ϕC31 *attB* site on the chromosome, yielding the corresponding gene deletion mutants *S. coelicolor* M1152/pCXF2 and *S. coelicolor* M1152/pCXF3.

trl. Single-gene-disruption mutants of the *trl* BGC in pCXF1 were constructed by λ-Red-mediated PCR targeting technology as described above. The identical procedure, using PCR-targeting primers ΔtrlA-F/R to ΔtrlR-F/R, was applied to delete genes *trlA* through *trlR* from pCXF1 individually, resulting in constructs pCXF4 to pCXF12. PCR analysis using primers ver-ΔtrlA-F/R to ver-ΔtrlR-F/R was used to confirm the single-gene-disruption constructs. pCXF4 through pCXF12 were introduced into *S. coelicolor* M1152 as described above, resulting in the single-gene-disruption mutants *S. coelicolor* M1152/pCXF4 through *S. coelicolor* M1152/pCXF12.

S. coelicolor 5 . Primers ΔpaaABCDE-F/R were used to probe pCXF13 from the cosmid genomic library of *S. coelicolor* M145 using cosmid DNA as the template. The *paaABCDE* genes on pCXF13 were deleted by λ-Red-mediated PCR targeting technology as described above, using ΔpaaABCDE-F/R targeting primers. The *paaABCDE* region on pCXF13 was then replaced by the *ermB* resistance cassette, resulting in the pCXF14 construct. pCXF14 was then transferred

Oligonucleotides used in this study

Oligonucleotide function and name	Sequence (5′→3′)[a]
Gene deletions by PCR targeting	
Δrib-F	GCCACCGCACCGCCGTACGGGCCGGGCCGCGGCCGTCCGatattccggggatccgtcgac
Δrib-R	GCGGCCGACGATCTGCTGGTGGACGTCGGCTTCCACGCCgtgtaggctggagctgcttc
Δshi-F	GCGACGGGTGCGACGGGTGCGGAACATGGGAGCGGCCCTatattccggggatccgtcgac
Δshi-R	GTGTGGCTCCGCCACGCCGTCCGCTCCGCGCTGACCCGGgtgtaggctggagctgcttc
ΔtrlA-F	GACCCCCGAGACGAAGGAGCACCCCCGTGCGGCACTTCGAGCACTatattccggggatccgtcgac
ΔtrlA-R	CCCGCTGGTTGTCCGCCTCGACGACGAACCGGACCGTGCCCGTGTtgtgtaggctggagctgcttc
ΔtrlB-F	GGAGATGGACGAGAACTCACTTGCCGATCCCTCTGTCGAAGCGTGatattccggggatccgtcgac
ΔtrlB-R	ACCTCGTCGCTCCCGCCCACGCACTCGGTGACGTCCTCCCCGGTGtgtgtaggctggagctgcttc
ΔtrlC-F	ACGAGTACCTGGAGAGCCTCCGGGACGGCCGGGAAGTCAGGATCTatattccggggatccgtcgac
ΔtrlC-R	CGTACTTGTCCAGGTAGGGCCGGACCTCGGGGTTGGACCAGTCGAtgtgtaggctggagctgcttc
ΔtrlD-F	GAGCCCCCGTCCTGCCGGACCAGGCCCAACTCAGGCACGTACTCGatattccggggatccgtcgac
ΔtrlD-R	GACAGCCGGTGTGCGGGCCGACGGCCCAGTCGGCGGCCTGCTCCAtgtgtaggctggagctgcttc
ΔtrlE-F	GACTGCGCAGGCAGGGCGTCGAGGCGGTCGTCCACGAGCAGGCGCatattccggggatccgtcgac
ΔtrlE-R	GTGCCAGGAAGTGGGCGAGGACCACCGCGTCCTCCAGGGCCTGGTtgtgtaggctggagctgcttc
ΔtrlF-F	ATGGCAAGGACCTACTCCTTCGAAGGCAACGTACCCGTCGTGCATatattccggggatccgtcgac
ΔtrlF-R	CTCGGTGGCGGCCTCCGCCGCGTGCAGACCGGTGAGACAGCGCTGtgtgtaggctggagctgcttc
ΔtrlG-F	CACCTCCCGACTCGTCGTCGGCGACCGGTTCCGCGACTTCGCCGAatattccggggatccgtcgac
ΔtrlG-R	CAGCGGGCCGTGAAGTAGCGCTCCACCACCGCGACGAACATCTGAtgtgtaggctggagctgcttc
ΔtrlH-F	ACCCGGAGTGGCGGTTCGCCTACCTGGGCCCGGAAGGAACCTTCAatattccggggatccgtcgac
ΔtrlH-R	CCAGGACTCTCAGTCCGGGCAGCCGCAGGCGCAGCAGGCCGACCGtgtgtaggctggagctgcttc
ΔtrlR-F	GACGTCGTCACCCCGCCCCCGTCGCGGCCGTGAGGACGTCCTCACatattccggggatccgtcgac
ΔtrlR-R	AGCAGCCGGGCGGCCAGGTGGGGAACGATGCCGTCGCGTATCTCGtgtgtaggctggagctgcttc
ΔpaaABCDE-F	CAGATCGCCCAGCACGCGCACTCGGAGATCATCGGCATGCAGattccggggatccgtcgacc
ΔpaaABCDE-R	GCAGGTCCCGCAGACCCCGCCCTTGCAGGCGAAGGGCAGGTCtgtaggctggagctgcttc
Verification of gene deletion mutants	
ver-Δrib-F	ATGTCACCGCTGCGCACCGA
ver-Δrib-R	ACCTCCGGTACGGACCAGGA
ver-Δshi-F	TCACGAACAGCTTCACCCACT
ver-Δshi-R	GGCATCGAACTGTTCGACCTT
ver-ΔtrlA-F	GACGACCGGTCCGGAGATCG
ver-ΔtrlA-R	CGGGTCGCCGAGTGGTTCAG
ver-ΔtrlB-F	GAAGGCCAGGTCCATCGACTG
ver-ΔtrlB-R	CTAGTACCCGGGTAGTAGATC
ver-ΔtrlC-F	CACCGGCTCGAAAGGTGATC
ver-ΔtrlC-R	GTAGTTCATCTCGTACAGCTC
ver-ΔtrlD-F	GAGTACGACGAGCACGGCTG
ver-ΔtrlD-R	CCTGTTCGCTGCCGAAGGC
ver-ΔtrlE-F	CCTTCACCGAAGTCGCACC
ver-ΔtrlE-R	CGACGCAGACGCTCGTAGG
ver-ΔtrlF-F	GATCCACGGGCACGACATC
ver-ΔtrlF-R	CGTCCTGACGGTCTTGTCC
ver-ΔtrlG-F	CACCGGACGTCACGTTCAGG
ver-ΔtrlG-R	CTCCGACTCGTCCACCGTCAG
ver-ΔtrlH-F	GTACGACGGTGGAGGTGGAA
ver-ΔtrlH-R	CGATGAGCAGGTGGTCCAGG
ver-ΔtrlR-F	GAGATCCAGCGGATCCGTAC
ver-ΔtrlR-R	GTCGTTCAGACGCCGCACC
ver-ΔpaaABCDE-F	GAGCACTTCGACGCGACGATC
ver-ΔpaaABCDE-R	GACTGGCAGGTCAGCACGTAG
paaABCDE-F	ATGACCACGACACACGCCGC
paaABCDE-R	CGCACCACCCAGATGCTCAC
Amplification of *t... l* genes for heterologous expression in *E. c... li*	
trlC-F	AAAGAATTCATGAGCAGCACCGTCAACC
trlC-R	AAAAAGCTTTCACCGTGCGGCCGGGCG
trlD-F	AAAGAATTCATGAGCAGCCACACCCCC
trlD-R	AAAAAGCTTTCACGGCGCCGGTGCGAC
trlE-F	AAAGAATTCATGGCGAGGAAACGCCCGTAC
trlE-R	AAAAAGCTTTCAGGCCGGTGACGTGGCCAC
trlB-F	AAAGAATTCGTGGAATCCCTGGAGATGGAC
trlB-R	AAAAAGCTTACTAGTTCAGCCGGGGGACGCCGCGTG
trlH-F	AAACATATGAGGACGCCGACACCGGAC
trlH-R	AAAAAGCTTACTAGTTCACCGTGGTGACCGCCCC

[a]Lowercase letters in sequences represent sequences that match with two boundaries of the erythromycin resistance gene cassette from pJTU6722.

into *S. coelicolor* M1152 by *E. coli*-*Streptomyces* triparental mating, and the DNA region encompassing *aaABCDE* on the chromosome was replaced by homologous double-crossover recombination, resulting in the *S. coelicolor* M1152 *aaABCDE* deletion strain *S. coelicolor* M1152P.

Streptomyces strains were cultured on SFM medium at 28 to 30°C for 4 to 6 days for sporulation. Then the *Streptomyces* spores were collected and were cultured on R3 agar petri dishes at 28 to 30°C for 4 to 6 days for metabolite production. R3 agar ferments were extracted three times with equal volumes of ethyl acetate (supplemented with 0.5% acetic acid), followed by concentration to dryness on a Buchi R-210 rotary evaporator at 35°C. The ethyl acetate extracts were first dissolved in methanol and then injected into an Agilent 1260 HPLC system for metabolic analysis on an Agilent Zorbax SB-C$_{18}$ column (particle size, 5 μm; inside diameter, 4.6 mm; length, 250 mm) using H$_2$O containing 0.1% trifluoroacetic acid (TFA) (solvent A) and 100% acetonitrile (ACN) (solvent B) as the mobile phase. The column was equilibrated with 95% solvent A and 5% solvent B. For HPLC elution, the following procedure was used: from 0 to 15 min, 5% to 40% B; from 15 to 25 min, 40% to 100% B; from 25 to 30 min, 100% B; from 31 to 38 min, 5% B. Elution was carried out at a rate of 0.6 ml/min at room temperature. The crude extracts were also injected into an HPLC-mass selective detector (MSD) trap mass spectrometer for recording the mass (range, *m/z* 50 to 500) using the same column and elution gradient with the electrospray ionization (ESI) source operated in positive mode. Agilent quadrupole time-of-flight (Q-TOF) G6530 mass spectrometry was used for recording the high-resolution mass of each compound, operating in ESI positive mode. The pure compounds were dissolved in methanol-d_4 or dimethyl sulfoxide (DMSO)-d_6 for recording NMR signals on the Avance III 600-MHz NMR spectrometer. X-ray crystallography data were collected on a single crystal X-ray diffractometer (Bruker Smart Apex) at the State Key Laboratory of Organometallic Chemistry in the Shanghai Institute of Organic Chemistry.

( ) A 3-liter R3 agar ferment of *S. coelicolor* M1152/pCXF1 was extracted three times with ethyl acetate (supplemented with 0.5% acetic acid) and was then concentrated under reduced evaporation at 35°C. The crude extract was then loaded onto a macroporous absorbent CHP20P resin column (diameter, 3.5 cm; length, 30 cm) and was eluted with an H$_2$O–CH$_3$OH gradient. The fractions were stored overnight at ambient temperature for crystallization, and brown crystals of compound 1 were obtained for subsequent HRMS and X-ray crystallography. The other compounds were obtained by identical procedures, with the exception of the details provided below.

( ) 0. A 3-liter R3 agar ferment of *S. coelicolor* M1152/pCXF7 (i.e., the Δ*ID* mutant) was used as the source. Brown crystals of compound 10 were obtained as described above and were used for HRMS, X-ray crystallography, and NMR analyses. NMR data are summarized in Table S1 in the supplemental material.

( ) A 10-liter R3 agar ferment of *S. coelicolor* M1152/pCXF6 (i.e., the Δ*IC* mutant) was used as the source. Fractions containing compound 8 were collected for crystallization and were stored at ambient temperature overnight. As with compounds 1 and 10, brown crystals were obtained for compound 8 for further HRMS and X-ray crystallography analyses. The fractions containing compound 9 were collected and were then applied to a YMC C$_{18}$ reversed-phase column (diameter, 2 cm; length, 20 cm) and were eluted with an H$_2$O–CH$_3$OH gradient (H$_2$O/CH$_3$OH ratios, 9:1, 17:3, 4:1, 7:3, 3:2, and 1:1). The fractions were monitored by HPLC using the method described under "Metabolic analysis" above. A pure sample of compound 9 (5 mg; elution at 20% methanol [MeOH]) was obtained for HRMS and NMR analyses.

( ) A 5-liter R3 agar ferment of *S. coelicolor* M1152/pCXF8 (i.e., the Δ*IE* mutant) was used as the source. HPLC fractions containing compound 11 or 12 were collected separately, concentrated to dryness under reduced evaporation at 35°C, and then applied to a YMC C$_{18}$ reversed-phase column (diameter, 2 cm; length, 20 cm) and eluted with an H$_2$O–CH$_3$OH gradient (H$_2$O/CH$_3$OH ratios, 19:1, 9:1, 4:1, 7:3, 3:2, 1:1, 2:3, 3:7, 1:4, and 1:9). The fractions were monitored by HPLC using the method described under "Metabolic analysis" above. Pure samples of compound 11 (5 mg; elution at 10% MeOH) and compound 12 (5 mg; elution at 60% MeOH) were collected for structural elucidation. Compound 11 was characterized by comparison to a pure standard and HRMS, whereas compound 12 was characterized by NMR analysis.

( ) A 5-liter R3 agar ferment of *S. coelicolor* M1152/pCXF9 (i.e., the Δ*IF* mutant) was used as the source. HPLC fractions containing compound 13 were collected, concentrated to dryness for subsequent fractionation on a YMC C$_{18}$ reversed-phase column (diameter, 2 cm; length, 20 cm), and eluted with an H$_2$O–CH$_3$OH gradient (H$_2$O/CH$_3$OH ratios, 7:3, 3:2, 1:1, 2:3, 3:7, 1:4, and 1:9). The fractions were monitored by HPLC using the method described under "Metabolic analysis" above. A pure sample of compound 13 (5 mg; elution at 80% MeOH) was obtained for HRMS and NMR analyses.

( ) , 4, 5, Compounds 3, 4, 5, and 6 were observed in the HPLC of R3 crude extracts of *S. coelicolor* M1152/pCXF10 (i.e., the Δ*IG* mutant), *S. coelicolor* M1152/pCXF11 (i.e., the Δ*IH* mutant), and *S. coelicolor* M1152/pCXF12 (i.e., the Δ*IR* mutant). Of these, *S. coelicolor* M1152/pCXF10 was selected to obtain compounds 3, 4, 5, and 6 for structural elucidation. A 5-liter R3 agar ferment of *S. coelicolor* M1152/pCXF10 was extracted, concentrated, and fractionated using the procedure described above for *S. coelicolor* M1152/pCXF1. The fractions were monitored by HPLC, and fractions containing compounds 3, 4, 5, and 6 were collected separately, concentrated to dryness for subsequent fractionation on a YMC C$_{18}$ reversed-phase column (diameter, 2 cm; length, 20 cm), and eluted with an H$_2$O–CH$_3$OH gradient (H$_2$O/CH$_3$OH ratios, 9:1, 4:1, 7:3, 3:2, 1:1, 2:3, 3:7, 1:4, and 1:9). The fractions were monitored by HPLC using the method described under "Metabolic analysis" above. Pure samples of compounds 3 (5 mg; elution at 60% MeOH), 4 (5 mg; elution at 40% MeOH), 5 (5 mg; elution at 40% MeOH), and 6 (5 mg; elution at 30% MeOH) were obtained. The fractions were stored overnight at ambient temperature for crystallization. White crystals of compound 3 were obtained.

S. coelicolor 5 / 5 . *S. c elic l* strain M1152/pCXF5 (i.e., the Δ *lB* mutant), which does not produce compound 1, was cultured on R3 agar petri dishes at 28 to 30°C for 2 days. A 200-μl volume of compound 7 dissolved in DMSO (2 mg/ml), was added, followed by 2 days of fermentation. Then 500 μl of compound 7 dissolved in DMSO (2 mg/ml) was added again, followed by a further 2 days of fermentation. R3 agar ferments were extracted three times with equal volumes of ethyl acetate (supplemented with 0.5% acetic acid), concentrated, and dissolved in methanol for HPLC analysis.

S. coelicolor 5 / 0 , , 0. *S. c elic l* strain M1152/pCXF10 (i.e., the Δ *lG* mutant), which does not produce compound 1, was inoculated into 30 ml TSBY seed medium and was incubated for 48 h with shaking at 220 rpm at 28 to 30°C. Then a 3-ml seed culture was inoculated into 30 ml R3 medium (10% seeding) in 250-ml baffled flasks. After 48 h of incubation at 28 to 30°C with shaking at 220 rpm, compounds 10 (3 mg), 8 (3 mg), and 11 (3 mg), dissolved in MeOH (300 μl), were added, followed by a further 4 days of fermentation. The R3 liquid ferments were then extracted with ethyl acetate (supplemented with 0.5% acetic acid), concentrated, and dissolved in methanol for HPLC analysis.

- **S. coelicolor** 5 / 0 . *S. c elic l* M1152/pCXF10 was inoculated in 30 ml TSBY seed medium for 48 h with shaking at 220 rpm at 28 to 30°C. Then a 3-ml seed culture was transferred into 30 ml R3 medium (10% seeding) in a 250-ml baffled flask. After a 4-day incubation at 28 to 30°C with shaking at 220 rpm, the mycelium was collected by centrifugation (6,000 × *g*, 10 min, 4°C) and was washed three times with 50 mM Tris-Cl buffer (pH 7.5). The washed mycelium was resuspended with 5 ml of 50 mM Tris-Cl buffer (pH 7.5), incubated with lysozyme (2 mg/ml) for 2 h at 30°C, and subsequently lysed by ultrasonication (Soniprep 150; Sanyo) in an ice bath. The lysed mycelium mixture was centrifuged at 12,000 × *g* for 10 min (4°C) to remove the cell debris, and the supernatant was transferred to a new 1.5-ml Eppendorf tube ready for use. Compounds 11 (100 μg) and 13 (100 μg), dissolved in 50 μl DMSO, were then added to the 1.5-ml Eppendorf tubes and were incubated in a 30°C water bath for 2 h. Then ethyl acetate (supplemented with 0.1% trifluoroacetic acid) was added to stop the reaction, and the reaction product was extracted three times for HPLC analysis.

- **E. coli** ( ) . The *lC* and *lD* genes were cloned into the pSJ7 and pSUMO vectors individually using primers trlC-F/R and trlD-F/R, respectively, resulting in the pCXF17 and pCXF18 constructs. pCXF17 and pCXF18 were transformed into *E. c li* strain BL21(DE3) to obtain the TrlC and TrlD expression strains *E. c li* BL21(DE3)/pCXF17 and *E. c li* BL21(DE3)/pCXF18, respectively. *lE* was cloned into pET-28a using primers trlE-F/R, resulting in the pCXF19 construct, which was then transformed into *E. c li* BL21(DE3) to obtain the TrlE expression strain *E. c li* BL21(DE3)/pCXF19.

A single colony of *E. c li* BL21(DE3)/pCXF17 was inoculated into 5 ml LB broth (with 50 mg/liter ampicillin) at 37°C, with shaking at 220 rpm overnight. A 1-ml *E. c li* culture was then transferred to 100 ml fresh LB broth (with 50 mg/liter ampicillin) and was incubated at 37°C with shaking at 220 rpm for 2 to 3 h, to an OD$_{600}$ of 0.4 to 0.6. IPTG was then added to a final concentration of 0.4 mM, and the culture was incubated at 16°C with shaking at 220 rpm for 16 to 20 h for protein expression. A 50-ml culture of *E. c li* BL21(DE3)/pCXF17 was pipetted into a 50-ml centrifuge tube, collected by centrifugation (10,000 × *g*, 10 min, 4°C), and washed three times with 50 mM Tris-HCl buffer (pH 7.5). The *E. c li* cells were resuspended with 1 ml of 50 mM Tris-HCl buffer (pH 7.5) and were subsequently lysed by ultrasonication (Soniprep 150; Sanyo) in an ice bath. The lysed cells were centrifuged at 12,000 × *g* for 10 min (4°C) to remove the cell debris, and the supernatant was transferred to a new 1.5-ml Eppendorf tube ready for use. An identical procedure was used to prepare an *E. c li* BL21(DE3)/pCXF18 cell extract. Compound 8 (100 μg) was dissolved in 50 μl DMSO, added to the cell-free mixtures of *E. c li* BL21(DE3)/pCXF17 and *E. c li* BL21(DE3)/pCXF18, and incubated at 30°C for 2 h. The cell-free reaction mixture was then extracted with ethyl acetate (supplemented with 0.1% trifluoroacetic acid) for subsequent HPLC analysis.

E. c li BL21(DE3)/pCXF19, expressing TrlE, was cultured and lysed like *E. c li* BL21(DE3)/pCXF17 for the cell-free experiment. Compound 1 (100 μg), dissolved in 50 μl DMSO, was then added to the supernatant of the *E. c li* BL21(DE3)/pCXF19 cell lysate and was incubated at 30°C for 2 h. The cell-free reaction mixture was then extracted with ethyl acetate (supplemented with 0.1% trifluoroacetic acid) for subsequent HPLC analysis as described.

. The 39-kb DNA sequence of pCXF1 was submitted to antiSMASH (46) and 2ndfind (http://biosyn.nih.go.jp/2ndfind/) for identification of biosynthetic gene clusters for natural products. A BLASTP search (https://blast.ncbi.nlm.nih.gov/Blast.cgi) against the GenBank nonredundant and UniProtKB/Swiss-Prot databases was used to annotate the proteins encoded on pCXF1. The 3,7-dihydroxytropolone biosynthetic gene cluster cloned from *S. l g i e* Slg41 is identical to the *S. c a e f c* Soc7 *l* BGC.

( ). Newly determined sequence data were deposited in the GenBank database under accession number MF955860.

Supplemental material for this article may be found at https://doi.org/10.1128/AEM.00349-18.

, PDF file, 2.2 MB.

1. Bentley R. 2008. A fresh look at natural tropolonoids. Nat Prod Rep 25:118–138. https://doi.org/10.1039/B711474E.
2. Grillo AS, SantaMaria AM, Kafina MD, Cioffi AG, Huston NC, Han M, Seo YA, Yien YY, Nardone C, Menon AV, Fan J, Svoboda DC, Anderson JB, Hong JD, Nicolau BG, Subedi K, Gewirth AA, Wessling-Resnick M, Kim J, Paw BH, Burke MD. 2017. Restored iron transport by a small molecule promotes absorption and hemoglobinization in animals. Science 356: 608–616. https://doi.org/10.1126/science.aah3862.
3. Metcalfe H, Field R, Froud S. 1994. The use of 2-hydroxy-2,4,6-cycloheptarin-1-one (tropolone) as a replacement for transferrin, p 88–90. *In* Spier RE, Griffiths JB, Berthold W, (ed), Animal cell technology: products of today, prospects for tomorrow. Butterworth-Heinemann, Oxford, United Kingdom.
4. Azegami K, Nishiyama K, Watanabe Y, Suzuki T, Yoshida M, Nose K, Toda S. 1985. Tropolone as a root growth-inhibitor produced by a plant pathogenic *Pseudomonas* sp. causing seedling blight of rice. Ann Phytopathol Soc Jpn 51:315–317. https://doi.org/10.3186/jjphytopath.51.315.
5. Sugawara K, Ohbayashi M, Shimizu K, Hatori M, Kamei H, Konishi M, Oki T, Kawaguchi H. 1988. BMY-28438 (3,7-dihydroxytropolone), a new antitumor antibiotic active against B16 melanoma. I. Production, isolation, structure and biological activity. J Antibiot (Tokyo) 41:862–868.
6. Didierjean J, Isel C, Querre F, Mouscadet JF, Aubertin AM, Valnot JY, Piettre SR, Marquet R. 2005. Inhibition of human immunodeficiency virus type 1 reverse transcriptase, RNase H, and integrase activities by hydroxytropolones. Antimicrob Agents Chemother 49:4884–4894. https://doi.org/10.1128/AAC.49.12.4884-4894.2005.
7. Piettre SR, Ganzhorn A, Hoflack J, Islam K, Hornsperger JM. 1997. α-Hydroxytropolone: a new class of potent inhibitors of inositol monophosphatase and other bimetallic enzymes. J Am Chem Soc 119: 3201–3204. https://doi.org/10.1021/ja9634278.
8. Donlin MJ, Zunica A, Lipnicky A, Garimallaprabhakaran AK, Berkowitz AJ, Grigoryan A, Meyers MJ, Tavis JE, Murelli RP. 2017. Troponoids can inhibit growth of the human fungal pathogen *Cryptococcus neoformans*. Antimicrob Agents Chemother 61:e02574-16. https://doi.org/10.1128/AAC.02574-16.
9. Li J, Falcone ER, Holstein SA, Anderson AC, Wright DL, Wiemer AJ. 2016. Novel alpha-substituted tropolones promote potent and selective caspase-dependent leukemia cell apoptosis. Pharmacol Res 113: 438–448. https://doi.org/10.1016/j.phrs.2016.09.020.
10. Meck C, D'Erasmo MP, Hirsch DR, Murelli RP. 2014. The biology and synthesis of alpha-hydroxytropolones. MedChemComm 5:842–852. https://doi.org/10.1039/C4MD00055B.
11. Cox RJ, Al-Fahad A. 2013. Chemical mechanisms involved during the biosynthesis of tropolones. Curr Opin Chem Biol 17:532–536. https://doi.org/10.1016/j.cbpa.2013.06.029.
12. Davison J, al Fahad A, Cai M, Song Z, Yehia SY, Lazarus CM, Bailey AM, Simpson TJ, Cox RJ. 2012. Genetic, molecular, and biochemical basis of fungal tropolone biosynthesis. Proc Natl Acad Sci U S A 109:7642–7647. https://doi.org/10.1073/pnas.1201469109.
13. Yan Y, Yang J, Yu Z, Yu M, Ma YT, Wang L, Su C, Luo J, Horsman GP, Huang SX. 2016. Non-enzymatic pyridine ring formation in the biosynthesis of the rubrolone tropolone alkaloids. Nat Commun 7:13083. https://doi.org/10.1038/ncomms13083.
14. Teufel R, Gantert C, Voss M, Eisenreich W, Haehnel W, Fuchs G. 2011. Studies on the mechanism of ring hydrolysis in phenylacetate degradation: a metabolic branching point. J Biol Chem 286: 11021–11034. https://doi.org/10.1074/jbc.M110.196667.
15. Teufel R, Mascaraque V, Ismail W, Voss M, Perera J, Eisenreich W, Haehnel W, Fuchs G. 2010. Bacterial phenylalanine and phenylacetate catabolic

pathway revealed. Proc Natl Acad Sci U S A 107:14390–14395. https://doi.org/10.1073/pnas.1005399107.
16. Brock NL, Nikolay A, Dickschat JS. 2014. Biosynthesis of the antibiotic tropodithietic acid by the marine bacterium *Phaeobacter inhibens*. Chem Commun (Camb) 50:5487–5489. https://doi.org/10.1039/c4cc01924e.
17. Wang R, Gallant É, Seyedsayamdost MR. 2016. Investigation of the genetics and biochemistry of roseobacticide production in the *Roseobacter* clade bacterium *Phaeobacter inhibens*. mBio 7:e02118-15. https://doi.org/10.1128/mBio.02118-15.
18. Xu M, Wang Y, Zhao Z, Gao G, Huang SX, Kang Q, He X, Lin S, Pang X, Deng Z, Tao M. 2016. Functional genome mining for metabolites encoded by large gene clusters through heterologous expression of a whole-genome bacterial artificial chromosome library in *Streptomyces* spp. Appl Environ Microbiol 82:5795–5805. https://doi.org/10.1128/AEM.01383-16.
19. Dosselaere F, Vanderleyden J. 2001. A metabolic node in action: chorismate-utilizing enzymes in microorganisms. Crit Rev Microbiol 27: 75–131. https://doi.org/10.1080/20014091096710.
20. Xun L, Sandvik ER. 2000. Characterization of 4-hydroxyphenylacetate 3-hydroxylase (HpaB) of *Escherichia coli* as a reduced flavin adenine dinucleotide-utilizing monooxygenase. Appl Environ Microbiol 66: 481–486. https://doi.org/10.1128/AEM.66.2.481-486.2000.
21. Jiménez JI, Canales A, Jiménez-Barbero J, Ginalski K, Rychlewski L, García JL, Díaz E. 2008. Deciphering the genetic determinants for aerobic nicotinic acid degradation: the *nic* cluster from *Pseudomonas putida* KT2440. Proc Natl Acad Sci U S A 105:11329–11334. https://doi.org/10.1073/pnas.0802273105.
22. Eichler K, Bourgis F, Buchet A, Kleber HP, Mandrand-Berthelot MA. 1994. Molecular characterization of the *cai* operon necessary for carnitine metabolism in *Escherichia coli*. Mol Microbiol 13:775–786. https://doi.org/10.1111/j.1365-2958.1994.tb00470.x.
23. Ferrández A, Miñambres B, García B, Olivera ER, Luengo JM, García JL, Díaz E. 1998. Catabolism of phenylacetic acid in *Escherichia coli*. Characterization of a new aerobic hybrid pathway. J Biol Chem 273:25974–25986.
24. Blakley ER. 1977. The catabolism of L-tyrosine by an *Alcaligenes* sp. Can J Microbiol 23:1128–1139. https://doi.org/10.1139/m77-169.
25. Mahanta N, Fedoseyenko D, Dairi T, Begley TP. 2013. Menaquinone biosynthesis: formation of aminofutalosine requires a unique radical SAM enzyme. J Am Chem Soc 135:15318–15321. https://doi.org/10.1021/ja408594p.
26. Van Lanen SG, Lin S, Shen B. 2008. Biosynthesis of the enediyne antitumor antibiotic C-1027 involves a new branching point in chorismate metabolism. Proc Natl Acad Sci U S A 105:494–499. https://doi.org/10.1073/pnas.0708750105.
27. Dastan A, Balci M. 2006. Chemistry of dioxine-annelated cycloheptatriene endoperoxides and their conversion into tropolone derivatives: an unusual non-benzenoid singlet oxygen source. Tetrahedron 62: 4003–4010. https://doi.org/10.1016/j.tet.2006.02.026.
28. Doering WVE, Detert FL. 1951. Cycloheptatrienylium oxide. J Am Chem Soc 73:876–877.
29. Grundmann C, Ottmann G. 1953. Preparation and structure of the isomeric cycloheptatriene carboxylic acids. Liebigs Ann Chem 582:15.
30. Citron CA, Barra L, Wink J, Dickschat JS. 2015. Volatiles from nineteen recently genome sequenced actinomycetes. Org Biomol Chem 13: 2673–2683. https://doi.org/10.1039/C4OB02609H.
31. Moore BS, Walker K, Tornus I, Handa S, Poralla K, Floss HG. 1997. Biosynthesis studies of ω-cycloheptyl fatty acids in *Alicyclobacillus cyc-*

phenylacetic. Formation of cycloheptanecarboxylic acid from phenylacetic acid. J Org Chem 62:2173–2185.

32. Rost R, Haas S, Hammer E, Herrmann H, Burchhardt G. 2002. Molecular analysis of aerobic phenylacetate degradation in *Azoarcus evansii*. Mol Genet Genomics 267:656–663. https://doi.org/10.1007/s00438-002-0699-9.

33. Thiel V, Brinkhoff T, Dickschat JS, Wickel S, Grunenberg J, Wagner-Döbler I, Simon M, Schulz S. 2010. Identification and biosynthesis of tropone derivatives and sulfur volatiles produced by bacteria of the marine *Roseobacter* clade. Org Biomol Chem 8:234–246. https://doi.org/10.1039/B909133E.

34. Chen L, Wang Y, Guo H, Xu M, Deng Z, Tao M. 2012. High-throughput screening for *Streptomyces* antibiotic biosynthesis activators. Appl Environ Microbiol 78:4526–4528. https://doi.org/10.1128/AEM.00348-12.

35. Datsenko KA, Wanner BL. 2000. One-step inactivation of chromosomal genes in *E. coli* K-12 using PCR products. Proc Natl Acad Sci U S A 97:6640–6645. https://doi.org/10.1073/pnas.120163297.

36. Gust B, Challis GL, Fowler K, Kieser T, Chater KF. 2003. PCR-targeted *Streptomyces* gene replacement identifies a protein domain needed for biosynthesis of the sesquiterpene soil odor geosmin. Proc Natl Acad Sci U S A 100:1541–1546. https://doi.org/10.1073/pnas.0337542100.

37. Flett F, Mersinias V, Smith CP. 1997. High efficiency intergeneric conjugal transfer of plasmid DNA from *E. coli* to methyl DNA-restricting streptomycetes. FEMS Microbiol Lett 155:223–229. https://doi.org/10.1111/j.1574-6968.1997.tb13882.x.

38. Bai T, Yu Y, Xu Z, Tao M. 2014. Construction of *Streptomyces lividans* SBT5 as an efficient heterologous expression host. J Huazhong Agric Univ 33:1–6.

39. Gomez-Escribano JP, Bibb MJ. 2011. Engineering *Streptomyces coelicolor* for heterologous expression of secondary metabolite gene clusters. Microb Biotechnol 4:207–215. https://doi.org/10.1111/j.1751-7915.2010.00219.x.

40. Li L, Xu Z, Xu X, Wu J, Zhang Y, He X, Zabriskie TM, Deng Z. 2008. The mildiomycin biosynthesis: initial steps for sequential generation of 5-hydroxymethylcytidine 5′-monophosphate and 5-hydroxymethylcytosine in *Streptoverticillium rimofaciens* ZJU5119. Chembiochem 9:1286–1294. https://doi.org/10.1002/cbic.200800008.

41. Zhao Z, Shi T, Xu M, Brock NL, Zhao YL, Wang Y, Deng Z, Pang X, Tao M. 2016. Hybrubins: bipyrrole tetramic acids obtained by crosstalk between a truncated undecylprodigiosin pathway and heterologous tetramic acid biosynthetic genes. Org Lett 18:572–575. https://doi.org/10.1021/acs.orglett.5b03609.

42. Peroutka RJ, III, Orcutt SJ, Strickler JE, Butt TR. 2011. SUMO fusion technology for enhanced protein expression and purification in prokaryotes and eukaryotes. Methods Mol Biol 705:15–30. https://doi.org/10.1007/978-1-61737-967-3_2.

43. Zhou J, Liu CY, Back SH, Clark RL, Peisach D, Xu Z, Kaufman RJ. 2006. The crystal structure of human IRE1 luminal domain reveals a conserved dimerization interface required for activation of the unfolded protein response. Proc Natl Acad Sci U S A 103:14343–14348. https://doi.org/10.1073/pnas.0606480103.

44. Kieser T, Bibb MJ, Buttner MJ, Chater KF, Hopwood DA. 2000. Practical *Streptomyces* genetics. The John Innes Foundation, Norwich, United Kingdom.

45. Shima J, Hesketh A, Okamoto S, Kawamoto S, Ochi K. 1996. Induction of actinorhodin production by *rpsL* (encoding ribosomal protein S12) mutations that confer streptomycin resistance in *Streptomyces lividans* and *Streptomyces coelicolor* A3(2). J Bacteriol 178:7276–7284. https://doi.org/10.1128/jb.178.24.7276-7284.1996.

46. Weber T, Blin K, Duddela S, Krug D, Kim HU, Bruccoleri R, Lee SY, Fischbach MA, Muller R, Wohlleben W, Breitling R, Takano E, Medema MH. 2015. antiSMASH 3.0—a comprehensive resource for the genome mining of biosynthetic gene clusters. Nucleic Acids Res 43:W237–W243. https://doi.org/10.1093/nar/gkv437.